Wilberforce pendulum oscillations and normal modes

Richard E. Berg and Todd S. Marshall
Lecture-Demonstration Facility, Department of Physics and Astronomy, University of Maryland, College Park, Maryland 20742

(Received 6 November 1989; accepted for publication 4 May 1990)

This article summarizes our calculation of the normal modes and the normal coordinates for a commercially available Wilberforce pendulum. A procedure is presented by which the normal coordinates may be produced experimentally, so that the frequencies of the normal modes can be obtained both theoretically and experimentally. Where possible, results have been compared with those from previous papers. Finally, PC BASIC programs have been written in which the behavior of the Wilberforce pendulum has been theoretically reproduced.

I. INTRODUCTION

The Wilberforce pendulum, named for its inventor, Lionel Robert Wilberforce,[1] Demonstrator in Physics at the Cavendish Laboratory, Cambridge, consists of a mass hanging on a flexible spiral spring that is free to oscillate in both the standard longitudinal mode and the torsional mode. Figure 1 is a drawing of one such Wilberforce pendulum. When the mass is lifted above its equilibrium point and released from rest, it oscillates up and down along a vertical line, slowly transferring its energy into a rotational oscillation. If the nuts screwed onto the vanes protruding from the sides of the mass are adjusted to give the appropriate moment of inertia such that the frequencies of the longitudinal mode and the torsional mode are the same, the pendulum will transfer its energy back and forth completely between these two modes of oscillation. Wilberforce was actually interested in the problem of determining the rigidity and the Young's modulus of various spring materials, and saw analysis of this coupling resonance as a technique to obtain more accurate values for Poisson's ratio more efficiently.

This device is well known as a demonstration of energy transfer and as a fascinating conversation piece. Sutton[2] discussed use of the Wilberforce pendulum as a demonstration of energy transfer between the longitudinal and the rotational modes. Geballe[3] presented an English summary of a then recent article in German by Krebs and Weidlich,[4] adding some of his own experimental data regarding the coupling between longitudinal and rotational oscillations which were obtained in the context of an advanced student laboratory. Freier and Anderson[5] described a pendulum which, in addition to the standard longitudinal and rotational modes, vibrates in a pendular mode with a frequency half that of the other two modes.[6–8] Williams and Keil[9] have discussed how a Wilberforce pendulum can be fabricated from spring wire, and present some observations made with one that they constructed. A standard laboratory and demonstration model is available commercially,[10] and a small version has been sold as an executive toy.[11] Another version described by Ehrlich[12] uses clay to adjust the moment of inertia and obtain resonance. A film loop[13] is available that simply shows the oscillation of a Wilberforce pendulum as it transfers back and forth between longitudinal and rotational modes.

The normal mode analysis of the Wilberforce pendulum is mentioned both in the original paper and in the paper by Geballe, but has not been discussed in detail. Although Geballe has determined the frequencies of the normal modes, no one has discussed the determination of the nor-

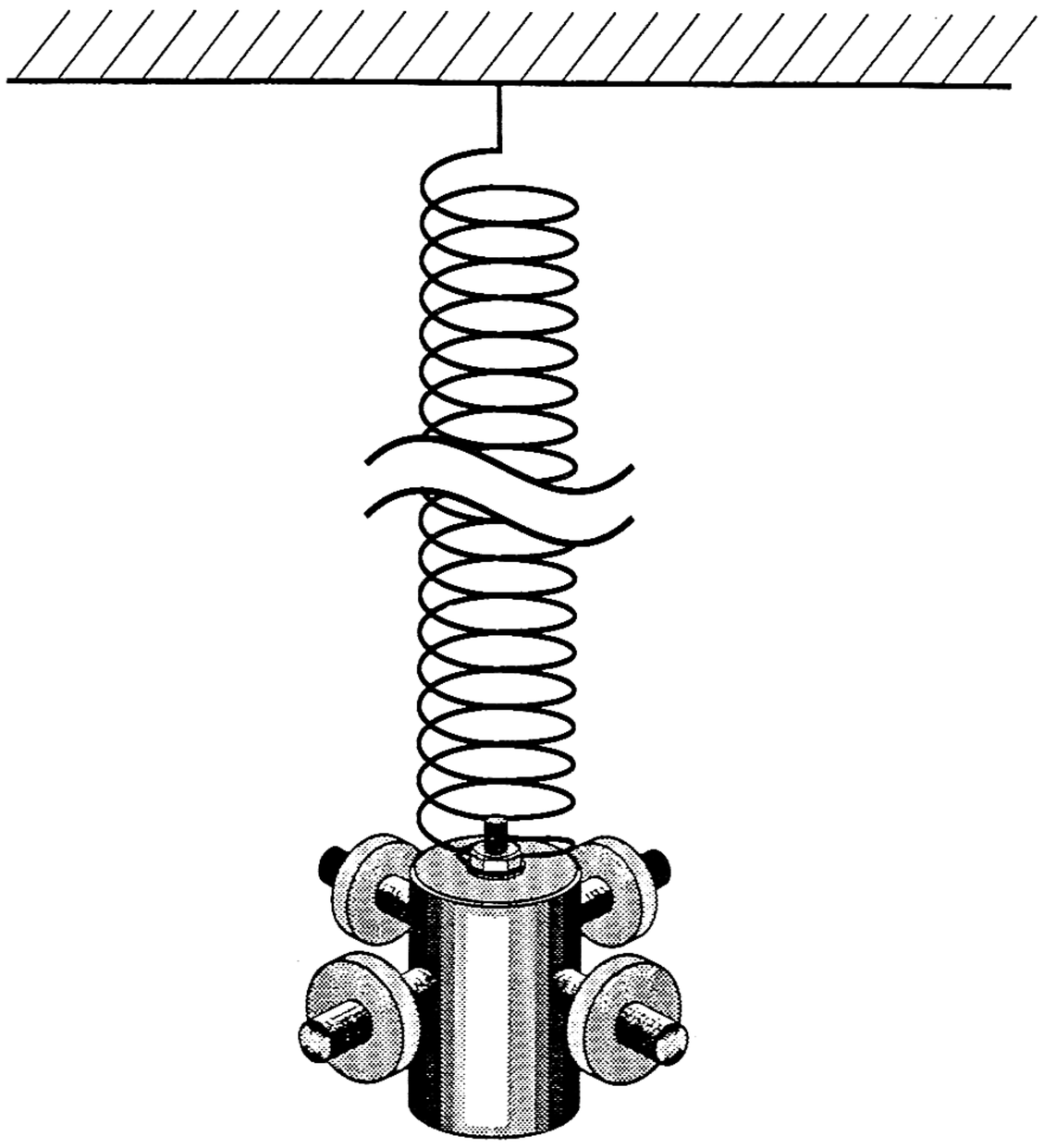

Fig. 1. Sketch of our Wilberforce pendulum. The actual length of the spring is almost 2 m.

mal coordinates or how they may be obtained in practice. We have carried out the complete normal mode analysis and have determined the coupling constant for our Wilberforce pendulum, from which we can experimentally obtain the normal coordinates and thus produce the normal modes. Because we have used a commercially available Wilberforce pendulum,[10] we feel that our data and our calculations will be particularly helpful to others interested in this device. We have solved the equations of motion analytically to obtain both the longitudinal and the rotational motion for any arbitrary initial conditions. In addition we have written a Runge–Kutta integration program for a PC which numerically integrates the equations of motion and plots both oscillation coordinates, allowing us to verify the important features of our theoretical treatment.

II. THEORY

A. Normal modes

Let us consider a massless spiral spring with a longitudinal spring constant k and a torsional spring constant δ, on which we hang a mass m with a moment of inertia I about its vertical axis. Assuming a linear coupling of the form $\epsilon z\theta/2$, where the two coordinates are z and θ, and $z=\theta=0$ is the equilibrium point, we can write the Lagrangian for the system as

$$L=\tfrac{1}{2}m\dot{z}^2+\tfrac{1}{2}I\dot{\theta}^2-\tfrac{1}{2}kz^2-\tfrac{1}{2}\delta\theta^2-\tfrac{1}{2}\epsilon z\theta, \tag{1}$$

where the first derivative with respect to time is notated by a single dot and the second derivative with respect to time by two dots.

The Lagrangian equations of motion for z and θ are then

$$m\ddot{z}+kz+\tfrac{1}{2}\epsilon\theta=0 \tag{2}$$

and

$$I\ddot{\theta}+\delta\theta+\tfrac{1}{2}\epsilon z=0, \tag{3}$$

where in the absence of the coupling term simple oscillations in z and θ are obtained. Eliminating z between Eqs. (2) and (3), and using the values for the frequencies $\omega_z^2=k/m$ and $\omega_\theta^2=\delta/I$,

$$\frac{d^4\theta}{dt^4}+(\omega_z^2+\omega_\theta^2)\frac{d^2\theta}{dt^2}+\left(\omega_z^2\omega_\theta^2-\frac{\epsilon^2}{4mI}\right)\theta=0, \tag{4}$$

where an equation of the same form exists for z.

Assuming a solution of the form

$$\theta(t)=Ae^{i\omega t}, \tag{5}$$

and inserting this into (4), we obtain a quartic equation,

$$\omega^4-(\omega_z^2+\omega_\theta^2)\omega^2+(\omega_z^2\omega_\theta^2-\epsilon^2/4mI)=0, \tag{6}$$

which can be solved to determine the frequencies of the normal modes,

$$\omega^2=\tfrac{1}{2}\{\omega_\theta^2+\omega_z^2\pm[(\omega_\theta^2-\omega_z^2)^2+\epsilon^2/mI]^{1/2}\}. \tag{7}$$

The frequencies of the two normal modes are then

$$\omega_1^2=\tfrac{1}{2}\{\omega_\theta^2+\omega_z^2+[(\omega_\theta^2-\omega_z^2)^2+\epsilon^2/mI]^{1/2}\}$$
$$=\omega^2+(\epsilon^2/4mI)^{1/2}, \tag{8}$$

and

$$\omega_2^2=\tfrac{1}{2}\{\omega_\theta^2+\omega_z^2-[(\omega_\theta^2-\omega_z^2)^2+\epsilon^2/mI]^{1/2}\}$$
$$=\omega^2-(\epsilon^2/4mI)^{1/2}, \tag{9}$$

when $\omega_\theta=\omega_z=\omega$. Using a binomial expansion for $\omega_B\ll\omega$ these solutions become

$$\omega_1=\omega+\epsilon/4\omega\sqrt{mI}=\omega+\omega_B/2 \tag{10}$$

and

$$\omega_2=\omega-\epsilon/4\omega\sqrt{mI}=\omega-\omega_B/2, \tag{11}$$

where we define

$$\omega_B=\epsilon/2\omega\sqrt{mI}, \tag{12}$$

in agreement with the result of Geballe. Here, $\omega_B=\omega_1-\omega_2$, the beat frequency between the two normal modes ω_1 and ω_2. This is analogous to the case of audible beats, where sinusoidal tones of nearby frequencies f_1 and $f_2<f_1$ with equal amplitudes combine to produce a tone of frequency $F=(f_1+f_2)/2$ beating at a rate $f_B=f_1-f_2$, so $f_1=F+f_B/2$ and $f_2=F-f_B/2$.

B. Normal coordinates

The general form of the rotation angle as a function of time will be a combination of the two normal modes above:

$$\theta(t)=A\sin\omega_1 t+B\cos\omega_1 t+C\sin\omega_2 t+D\cos\omega_2 t, \tag{13}$$

so

$$\ddot{\theta}(t)=-A\omega_1^2\sin\omega_1 t-B\omega_1^2\cos\omega_1 t$$
$$-C\omega_2^2\sin\omega_2 t-D\omega_2^2\cos\omega_2 t, \tag{14}$$

where A and B are the amplitudes of sine and cosine components for mode 1 and C and D are those for mode 2.

Substituting Eqs. (13) and (14) into Eq. (3) above, we obtain the general equation for z as a function of time:

$$z(t) = (2I\omega_1^2/\epsilon)(A\sin\omega_1 t + B\cos\omega_1 t) + (2I\omega_2^2/\epsilon)(C\sin\omega_2 t + D\cos\omega_2 t) - (2\delta/\epsilon)(A\sin\omega_1 t + B\cos\omega_1 t + C\sin\omega_2 t + D\cos\omega_2 t), \quad (15)$$

from which

$$\dot{z}(t) = (2I\omega_1^2/\epsilon)(A\omega_1\cos\omega_1 t - B\omega_1\sin\omega_1 t) + (2I\omega_2^2/\epsilon)(C\omega_2\cos\omega_2 t - D\omega_2\sin\omega_2 t) - (2\delta/\epsilon)(A\omega_1\cos\omega_1 t - B\omega_1\sin\omega_1 t + C\omega_2\cos\omega_2 t - D\omega_2\sin\omega_2 t). \quad (16)$$

From the initial conditions, where the pendulum is given an initial vertical displacement and an initial twist, but no initial velocity in either coordinate,

$$z(0) = z_0,\ \dot{z}(0) = 0,\ \theta(0) = \theta_0,\ \dot{\theta}(0) = 0, \quad (17)$$

we obtain values for the amplitudes A, B, C, and D:

$$A = C = 0, \quad (18)$$

$$B = (\omega_1^2 - \omega_2^2)^{-1}[\epsilon z_0/2I - (\omega_2^2 - \omega_\theta^2)\theta_0] \quad (19)$$

and

$$D = -(\omega_1^2 - \omega_2^2)^{-1}[\epsilon z_0/2I - (\omega_1^2 - \omega_\theta^2)\theta_0]. \quad (20)$$

Thus

$$\theta(t) = (\epsilon z_0/2I)(\omega_1^2 - \omega_2^2)^{-1}(\cos\omega_1 t - \cos\omega_2 t) + \theta_0(\omega_1^2 - \omega_2^2)^{-1}[(\omega_1^2 - \omega_\theta^2)\cos\omega_2 t - (\omega_2^2 - \omega_\theta^2)\cos\omega_1 t] \quad (21)$$

and

$$z(t) = z_0(\omega_1^2 - \omega_2^2)^{-1}[(\omega_1^2 - \omega_\theta^2)\cos\omega_1 t - (\omega_2^2 - \omega_\theta^2)\cos\omega_2 t] - (2I\theta_0/\epsilon)(\omega_1^2 - \omega_2^2)^{-1}(\omega_1^2 - \omega_\theta^2)(\omega_2^2 - \omega_\theta^2) \times (\cos\omega_1 t - \cos\omega_2 t). \quad (22)$$

This motion is a linear combination of the two normal modes

$$\mathbf{X}(t) = z(t)\hat{z} + \theta(t)\hat{\theta} = A_1\hat{\eta}_1\cos\omega_1 t + A_2\hat{\eta}_2\cos\omega_2 t, \quad (23)$$

where $\hat{\eta}_1$ and $\hat{\eta}_2$ are the normal coordinates that we must determine, and $\hat{z}$ and $\hat{\theta}$ are "unit vectors" for the longitudinal and the torsional motion. Substituting Eqs. (21) and (22) into Eq. (23), and separating out factors of $\cos\omega_1 t$ and $\cos\omega_2 t$, we can identify the amplitudes

$$A_1 = (\omega_1^2 - \omega_2^2)^{-1}[\epsilon z_0/2I - (\omega_2^2 - \omega_\theta^2)\theta_0] \quad (24)$$

and

$$A_2 = -(\omega_1^2 - \omega_2^2)^{-1}[\epsilon z_0/2I - (\omega_1^2 - \omega_\theta^2)\theta_0], \quad (25)$$

and the normal coordinates

$$\hat{\eta}_1 = \hat{\theta} + (2I/\epsilon)(\omega_1^2 - \omega_\theta^2)\hat{z} \quad (26)$$

and

$$\hat{\eta}_2 = \hat{\theta} + (2I/\epsilon)(\omega_2^2 - \omega_\theta^2)\hat{z}. \quad (27)$$

From Eq. (23), the condition for obtaining mode 1 is that $A_2 = 0$, and the condition for obtaining mode 2 is that $A_1 = 0$. Thus we obtain the relation between z_0 and θ_0 for the normal coordinates,

$$z_0 = (2I/\epsilon)(\omega_1^2 - \omega_\theta^2)\theta_0 = +\sqrt{I/m}\,\theta_0 \quad \text{(mode 1)} \quad (28)$$

and

$$z_0 = (2I/\epsilon)(\omega_2^2 - \omega_\theta^2)\theta_0 = -\sqrt{I/m}\,\theta_0 \quad \text{(mode 2)}, \quad (29)$$

where we have substituted for ω_1 and ω_2 using Eqs. (8) and (9), and used $\omega_\theta = \omega$.

Also from Eqs. (10) and (11) the coupling constant can be determined,

$$\epsilon = (\omega_1^2 - \omega_2^2)\sqrt{mI} = 2\omega\omega_B\sqrt{mI}. \quad (30)$$

The moment of inertia and the mass of the pendulum bob are related by its radius of gyration Γ,

$$I = m\Gamma^2, \quad (31)$$

so Eqs. (28) and (29) become

$$z_0 = +\Gamma\theta_0 \quad \text{(mode 1)} \quad (32)$$

and

$$z_0 = -\Gamma\theta_0 \quad \text{(mode 2)}. \quad (33)$$

III. EXPERIMENTAL MEASUREMENTS

We used the Leybold–Heraeus "Wilberforce's pendulum," available from Central Scientific Company.[10] The only physical specifications given are "The pendulum consists of a 30-mm-wide helical spring, made of 1-mm-thick steel wire and having 140 to 150 turns." By actual count the number of turns is 130, and our measurements show the coil diameter to be 30.7 mm to the center of the wires. Physical specifications for the coil are summarized in Table I.

The mass and the moment of inertia of our pendulum bob in its proper configuration were determined independently to be

$$m = 0.4905 \pm 0.0003\ \text{kg},$$

$$I = 1.39 \pm 0.02 \times 10^{-4}\ \text{kg m}^2.$$

We determined the moment of inertia by taking the bob apart, measuring the masses and dimensions of its components, and calculating the moment of inertia from these measurements. We also determined the moment of inertia using a small torsional oscillator.[14] The frequency was measured with a cylindrical base of known moment of inertia and again with the pendulum bob added to the base, from which the moment of inertia of the bob about its vertical axis was determined. These two methods were in general agreement, but the former technique seemed to be more accurate.

Table I. Physical parameters for a spring.

Coil radius R	1.535 cm
Wire diameter d	1.0 mm
Number of turns n	130
Pitch unloaded (tight)	1.0 mm
Pitch h loaded	1.4 cm
Pitch angle α loaded	8.35°
Steel parameters	
Shear modulus G	8.1×10^{10} Pa
Poisson's ratio σ	0.23

These values must be corrected for the mass and the moment of inertia of the spring, respectively, to obtain optimum accuracy. This problem has been discussed in great detail by a number of authors, including Edwards and Hultsch,[15] who described nonlinear effects in a vibrating vertical spring. Fox and Mahanty[16] showed that, in the limit where the spring mass is negligible in comparison with the mass of the bob, the correction is equal to one-third of the mass of the spring. Further information for both the static and the dynamic cases is provided by Galloni and Kohen,[17] as well as the references in the two preceding articles. Sommerfeld[18] gives the same factor of one-third as the limiting case for the correction to the moment of inertia due to the moment of inertia of the spring.

In our case, using Eq. (7) from Edwards and Hultsch we obtain the correction

$$m_{\text{corr}} = m + 0.337\ m_{\text{spring}}, \tag{34}$$

so

$$I_{\text{corr}} = I + 0.337 I_{\text{spring}}, \tag{35}$$

where the moment of inertia of the spring is taken about its axis. In this case the moment of inertia of the spring was calculated from its measured mass and radius. The final values are

$$m_{\text{spring}} = 0.0768 \pm 0.0002\ \text{kg}$$

and

$$I_{\text{spring}} = 0.181 \pm 0.005 \times 10^{-4}\ \text{kg m}^2,$$

so

$$m_{\text{corr}} = 0.5164 \pm 0.0004\ \text{kg},$$

$$I_{\text{corr}} = 1.45 \pm 0.02 \times 10^{-4}\ \text{kg m}^2.$$

Thus the relation between the twist and the vertical displacement to obtain the normal coordinates for our Wilberforce pendulum is

$$z_0 = +0.0168 \pm 0.0002\theta_0 \quad \text{(mode 1)} \tag{36}$$

and

$$z_0 = -0.0168 \pm 0.0002\theta_0 \quad \text{(mode 2)}, \tag{37}$$

where θ_0 is in radians and z_0 is in meters, so the two normal coordinates are obtained by giving each a vertical displacement followed by either a clockwise or a counterclockwise rotation.

In practice, we rotated the system by one full turn (an easily determined rotation), in either direction, and lifted it by the amount determined using Eqs. (36) and (37). The normal modes were very stable, and could be observed for several minutes as the motion simply damped down with no discernible transfer of the energy between the original longitudinal and torsional modes.

The instruction sheet for the Leybold–Heraeus "Wilberforce's pendulum" suggests that one technique in adjusting the moment of inertia to obtain the resonance condition is "... the spring is twisted in its position of rest by turning the weight about its own axis once, the weight is then lifted about 10 cm high and released. Under these circumstances, there is no phase shift between the longitudinal and torsional oscillations which, therefore, do not affect one other in the beginning." The calculation above leading to Eqs. (36) and (37) shows that this is a reasonable suggestion and lays out its theoretical basis.

The correction to Γ in Eqs. (34) and (35) due to the effects of the spring is small:

$$\Gamma^2 = \frac{I_{\text{corr}}}{m_{\text{corr}}} = \frac{I}{m}\left[1 + \frac{m_s}{3m}\left(\frac{R^2}{\Gamma^2} - 1\right) - \cdots .\right],$$

which is less than 1% after taking the square root. The difference between Γ obtained using corrected and uncorrected values of I and m in our case is indeed less than 1%, and well within the limit that can be observed when experimentally setting up the normal modes.

The measured frequencies in the energy-transfer mode are

$$\omega = \omega_\theta = \omega_z = 2.31 \pm 0.02\ \text{rad/s}$$

and

$$\omega_B = 0.232 \pm 0.002\ \text{rad/s}.$$

The frequencies that we measured for the normal modes are close to those expected from the calculation using the measured longitudinal/torsional oscillation frequency ω and the measured beat frequency ω_B:

$$\omega_1 = \omega + \omega_B/2 = 2.43 \pm 0.02\ \text{rad/s} \quad \text{(calculated)},$$

$$\omega_1 = 2.41 \pm 0.01\ \text{rad/s} \quad \text{(measured directly)},$$

for the mode in which the spring is lifted and unwound, and

$$\omega_2 = \omega - \omega_B/2 = 2.19 \pm 0.02\ \text{rad/s} \quad \text{(calculated)},$$

$$\omega_2 = 2.18 \pm 0.01\ \text{rad/s} \quad \text{(measured directly)},$$

for the mode in which the spring is lifted and wound more tightly.

Using our measured normal mode frequencies

$$\omega_B = \omega_1 - \omega_2$$

$$= 0.23 \pm 0.01\ \text{rad/s} \quad \text{(from normal modes)}.$$

We also performed static measurements of the longitudinal spring constant k and the torsional spring constant δ,

$$k = 2.80 \pm 0.05\ \text{N/m}$$

and

$$\delta = 7.86 \pm 0.16 \times 10^{-4}\ \text{N m},$$

from which the standard oscillation frequencies can be determined:

$$\omega_z = \sqrt{k/m} = 2.33 \pm 0.02\ \text{rad/s}$$

and

$$\omega_\theta = \sqrt{\delta/I} = 2.33 \pm 0.04\ \text{rad/s},$$

using the corrected values for m and I.

IV. COMPARISON WITH SOMMERFELD THEORY

We can obtain further insight into the nature of this resonant system by comparing our results with those obtained by Sommerfeld,[18] in a treatment that approaches the problem from first principles of spring construction. Sommerfeld's equations, modified to our notation, are

$$\ddot{z} + \omega_z^2 z + (kR/m)(\sigma \sin\alpha \cos\alpha)\theta = 0 \tag{38}$$

and

$$\ddot{\theta} + \omega_\theta^2 \theta + (kR/I)(\sigma \sin\alpha \cos\alpha) z = 0, \tag{39}$$

with the spring constant for negligible pitch

$$k = GJ_p/R^2\ell \tag{40}$$

and the polar moment of inertia of the wire

$$J_p = \pi d^4/32, \tag{41}$$

where σ is Poisson's ratio, α is the slope of the spring helix for a coil of radius R constructed from wire of diameter d and total length ℓ using material of shear modulus G. Thus the theoretical value for our longitudinal and torsional spring constants are

$$k = Gd^4/64nR^3 = 2.69 \text{ N/m}$$

and

$$\delta = kR^2(1+\sigma\cos^2\alpha) = 7.77 \pm 0.01\times 10^{-4} \text{ N m},$$

where n is the number of turns in the spring. Here we have used the value $G = 8.1\times 10^{10}$ Pa for the shear modulus,[19] and measured values for the coil radius R, the wire diameter d, the number of turns n, and the pitch h of the loaded spring. For our case the pitch h of the loaded spring is 1.4 cm so the angle

$$\alpha = 0.1457 \pm 0.0004,$$

where $\sin\alpha = h/(2\pi R)$.

Using Sommerfeld's relations we can also determine the values of the longitudinal and the rotational frequencies, corrected for details of the spring structure:

$$\omega_z^2 = (GJ_p/mR^2\ell)(1+\sigma\sin^2\alpha)$$
$$= (k/m)(1+\sigma\sin^2\alpha) \quad (42)$$

and

$$\omega_\theta^2 = (GJ_p/I\ell)(1+\sigma\cos^2\alpha)$$
$$= (kR^2/I)(1+\sigma\cos^2\alpha), \quad (43)$$

from which

$$\omega_z = 2.288 \pm 0.001 \text{ rad/s}$$

and

$$\omega_\theta = 2.31 \pm 0.02 \text{ rad/s},$$

using $\sigma = 0.23$,[19] the theoretical value for k, the measured value for α, and corrected measured values for m and I.

It is interesting to use the resonance condition by setting the two frequencies of Eqs. (42) and (43) equal:

$$(k/m)(1+\sigma\sin^2\alpha) = (kR^2/I)(1+\sigma\cos^2\alpha), \quad (44)$$

from which, using $I = m\Gamma^2$, we obtain

$$\Gamma = R\,[(1+\sigma\cos^2\alpha)/(1+\sigma\sin^2\alpha)]^{1/2}. \quad (45)$$

For small α this reduces to

$$\Gamma = R(1+\sigma)^{1/2}, \quad (46)$$

a result also given by Feather,[20] the following a derivation along the lines of Sommerfeld's.

Using our measured value for α, this becomes

$$\Gamma = 1.10R,$$

which can be compared with our experimental value of

$$\Gamma = 1.09R,$$

using the value for the radius of gyration from Eqs. (36) and (37) and a coil radius of 0.015 35 m.

Thus any pendulum bob whose radius of gyration is related to the coil radius by Eq. (45) should be at resonance, within the limits of small pitch angle inherent in the Sommerfeld theory.

V. COMPUTER CALCULATIONS

Equations (21) and (22) can be solved to obtain the position and the rotation of the bob as a function of time if the bob is displaced from its vertical equilibrium point and/or given some rotation. Alternatively, Eqs. (2) and (3) can be numerically integrated to obtain the bob position and rotation as a function of time. Both of the above procedures gave the same result, a condition which we used to check our mathematics. Figure 2 shows both z and θ as a function of time for one complete beat oscillation when the bob is raised and released from rest, obtained by numerically integrating Eqs. (2) and (3) using a Runge–Kutta technique,[21] details of which will be described later.

One characteristic of a system in which the coupling is linear and which therefore possesses normal modes is that the motion of the system in a normal mode always lies along a line for any amplitude, in this case one of the two lines given by $z = \pm 0.0168\theta$. This may be contrasted with the case of the elastic pendulum, for which the coupling is nonlinear, leading to stable oscillations which have different paths in z-θ space for each amplitude. Another interesting observation is the relationship between the phases of the z or the θ motion as the energy transfer is completed and restarted, as can be observed in Fig. 2. Completing the analogy to audible beats, this phase behavior is identical to that of the waveform for audible beats, which is obtained by balanced modulation (or double-sideband modulation or ring modulation) of the average frequency F by the frequency $f_B/2$.[22] In the case of the Wilberforce pendulum the beating is between the two normal modes ω_1 and ω_2. Inspection of the graph of the motion, as well as the equations for z and θ presented in our development, also reinforces the meaning of z and θ as truly equivalent and symmetrical canonical variables.

Our introduction of ϵ as an operational coupling constant provides us with additional insight into this system and illustrates the limit of the Sommerfeld treatment.

From Eq. (30), using our measured ω, ω_B, m, and I,

$$\epsilon = 2\omega\omega_B\sqrt{mI} = 9.27 \pm 0.30\times 10^{-3} \text{ N}.$$

Equations (2) and (3) can be put in canonical form,

$$\frac{d\dot{z}}{dt} = -\omega^2 z - \frac{\epsilon}{2m}\theta, \quad \frac{dz}{dt} = \dot{z} \quad (47)$$

and

$$\frac{d\dot{\theta}}{dt} = -\omega^2\theta - \frac{\epsilon}{2I}z, \quad \frac{d\theta}{dt} = \dot{\theta}, \quad (48)$$

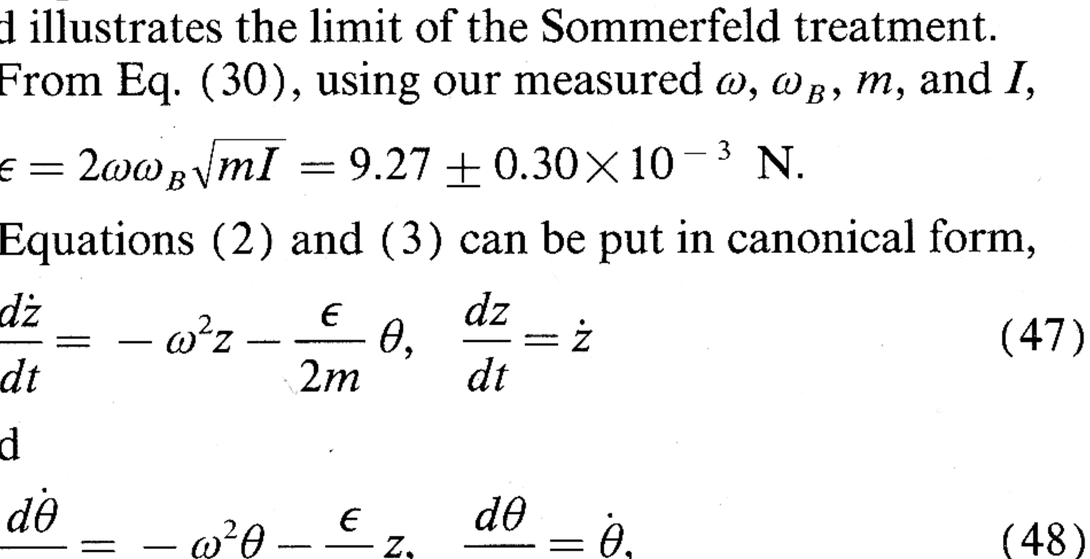

Fig. 2. Coordinates z and θ as a function of time for our Wilberforce pendulum, when the pendulum is started in the longitudinal mode by lifting the bob straight up and releasing it from rest.

for Runge–Kutta integration. For the value of ϵ obtained above, the values of ω, the pure longitudinal or torsional oscillation frequency, ω_1 and ω_2, the normal mode frequencies, and ω_B, the beat frequency were determined by inspection of the computed oscillations. The values obtained are

$$\omega = \omega_z = \omega_\theta = 2.314 \text{ rad/s},$$

$$\omega_B = 0.2315 \text{ rad/s},$$

$$\omega_1 = 2.424 \text{ rad/s},$$

$$\omega_2 = 2.191 \text{ rad/s},$$

which are consistent with our experimental results.

In most respects, the Sommerfeld treatment and our treatment are complementary; however, in the case of the value of the coupling constant ϵ, our results deviate significantly. We believe that this is because of the inherent limit of the Sommerfeld theory to "small pitch angles," as discussed above. Our parameter ϵ is related to the energy content of the spring, and is clearly greater with the larger bob mass than that assumed in the Sommerfeld derivation. As a result of this difference we cannot independently determine σ. In addition, using both ϵ values in our numerical integration shows that our results are quite consistent, while the value for ϵ predicted by the Sommerfeld theory produces incorrect oscillation frequencies for the pendulum.

Comparison of our Eqs. (2) and (3) with Sommerfeld's Eqs. (38) and (39) above allows us to make the identification

$$\epsilon = kR\sigma \sin 2\alpha \tag{49}$$

from which

$$\epsilon = 2.73 \pm 0.01 \times 10^{-3} \text{ N},$$

using theoretical values for k and σ, and measured values for R and α.

Adjusting the value of ϵ in differential equations (47) and (48) above results in substantially different oscillation frequencies for the normal modes. For example, if $\epsilon = 2.89 \times 10^{-3}$ N, then

$$\omega = \omega_z = \omega_\theta = 2.310 \text{ rad/s},$$

$$\omega_B = 0.068 \text{ rad/s},$$

$$\omega_1 = 2.344 \text{ rad/s},$$

$$\omega_2 = 2.276 \text{ rad/s},$$

which are consistent with themselves but deviate significantly from all of our other results.

While our use of ϵ as an operational variable for the purpose of determining the normal modes and normal coordinates works as long as the coupling between modes is linear, Sommerfeld's treatment cannot be extended to this general case, because of the additional forces due to twisting and bending of the spring under the applied weight. This is consistent with Sommerfeld's introductory statement on p. 308, regarding the winding of his spring, "On removing the mandrel, we obtain a helical spring which we fasten at one end in some way, loading the other end with a disk, the weight of which is supposed to be small enough so that the resulting pitch of the spring is *small* compared to the radius of the cylinder." In the present case, although the pitch is equal to the wire diameter for the unloaded coil, the radius is about 1.5 cm and the pitch is over 1.4 cm with the mass added, so Sommerfeld's condition does not apply. For our treatment no such limitation applies, as long as the coupling is linear.

VI. SUMMARY AND CONCLUSIONS

The procedure that we have suggested yields good results for determination and experimental verification of both normal modes and normal coordinates. Our equations differ from those of Sommerfeld in that there is no limit on the stretch of the coil within the constraints of linearity of ϵ. Determination of Poisson's ratio σ has been the primary goal in use of the Wilberforce pendulum, with Wilberforce (and Geballe) using coupling between the longitudinal and the torsional modes and Sommerfeld proposing a technique more directly related to the resonance. However, our aim in this paper is to show how the normal coordinates of the Wilberforce pendulum can be set up and to verify this procedure both experimentally and by comparison with computed oscillations. For very light masses, the value of ϵ obtained in Eq. (30) could be used in Eq. (49) to determine σ. However, both commercial Wilberforce systems and those constructed by physicists, as described in the literature, use larger masses, and therefore lie outside of the limits specified by the Sommerfeld treatment.

Note added in proof: In a paper published after acceptance of this manuscript, Köpf [23] stated that, once the resonance condition $\omega_\theta = \omega_z$ has been met, then "With the pendulum thus tuned, one can demonstrate experimentally the rather astonishing fact that neither length or diameter of the wire nor pitch and number of turns influences the resonant condition." Equations (32) and (33) constitute a theoretical basis for that conclusion in that they are derived directly from the resonance condition and involve only the radius of gyration Γ of the pendulum bob explicitly. In fact, using Sommerfeld's approach to obtain Eqs. (45) and (46), it is clear that the only factors that affect the resonant value of the radius of gryation are the pitch, coil radius, and Poisson's ratio. In the limit of small pitch angle, the only spring parameters which have any influence whatever on the resonant condition are coil radius R and Poisson's ratio σ. This is why the Wilberforce pendulum was valuable in experimental determination of Poisson's ratio.

ACKNOWLEDGMENTS

We would like to thank an anonymous reviewer for his very insightful and constructive suggestions during the review process. We would also like to thank Geoffrey Elbo and Joan Wright Hamilton for their help in preparing the figures.

[1] L. R. Wilberforce, "On the vibrations of a loaded spiral spring," Philos. Mag. **38**, 386–392 (1894).

[2] Richard Manliffe Sutton, *Demonstration Experiments in Physics* (McGraw-Hill, New York, 1938), Experiment S-18, "Transfer of energy from translation to rotation," p. 135, out of print but reprinted with permission by Kinko's Copies, 114 W. Franklin St., Chapel Hill, NC 27516.

[3] Ronald Geballe, "Statics and dynamics of a helical spring," Am. J. Phys. **26**, 287–290 (1958).

[4] Karl Krebs and Wolfgang Weidlich, "Zur Theorie der Schraubenfer," Z. Angew. Phys. **5**, 260–267 (1953).

[5] G. D. Freier and F. J. Anderson, *A Demonstration Handbook for Physics* (American Association of Physics Teachers, College Park, MD, 1981) Demonstration Mx-11, "Wilburforce [sic] Pendulum," p. M-61.

[6] M. G. Olsson, "Why does a spring sometimes misbehave?," Am. J. Phys. **44**, 1211–1212 (1976).

[7] J. G. Lipham and V. L. Pollak, "Constructing a misbehaving spring," Am. J. Phys. **46**, 110–111 (1978).

[8] M. G. Rusbridge, "Motion of the spring pendulum," Am. J. Phys. **48**, 146–151 (1980).

[9] Jim Williams and Rudy Keil, "A Wilberforce pendulum," Phys. Teach. **21**, 257–258 (1983).

[10] Leybold-Heraeus 346 51 Wilberforce's pendulum, available from Central Scientific Company, Chicago, IL.

[11] B & B Co., Wauwatosa, WI, Super Spinnerama.

[12] Robert Ehrlich, *Turning the World Inside Out and* 174 *Other Simple Physics Demonstrations* (Princeton U. P., Princeton, NJ, 1990), Demonstration G. 1, Wilburforce [sic] pendulum, pp. 89–90.

[13] Wilberforce Pendulum, Catalog #80-2157 from the film loop series Demonstrations in Physics, by Franklin Miller, Kenyon College, originally published by Ealing Film Loops, now available from Kalmia Co., Inc., Department A2, 71 Dudley Street, Cambridge, MA 02140.

[14] We used the Klinger 11 0611 Small Rotator on Rod with the disk from the Klinger 11 0632 Wooden disk and sphere as a base to make our moment of inertia measurements.

[15] T. W. Edwards and R. A. Hultsch, "Mass distribution and frequencies of a vertical spring," Am. J. Phys. **40**, 445–449 (1972).

[16] J. G. Fox and J. Mahanty, "The effective mass of an oscillating spring," Am. J. Phys. **38**, 98–100 (1970).

[17] Ernesto E. Galloni and Mario Kohen, "Influence of the mass of the spring on its static and dynamic effects," Am. J. Phys. **47**, 1076–1078 (1979).

[18] Arnold Sommerfeld, *Mechanics of Deformable Bodies: Lectures on Theoretical Physics* (Academic, New York, 1950), Vol. II, pp. 308–314, translated from the second German edition by G. Kuerti, Harvard University.

[19] Jerry B. Marion and William F. Hornyak, *Physics For Science and Engineering, Part I* (Saunders College Publishing, New York, 1982), pp. 437–441.

[20] Norman Feather, *Vibrations and Waves* (Penguin, Baltimore, MD, 1964), pp. 59–67.

[21] Michael J. Romanelli, "Runge–Kutta methods for the solution of ordinary differential equations," in *Mathematical Methods for Digital Computers*, edited by Anthony Ralston and Herbert S. Wilf (Wiley, New York, 1964), pp. 110–120.

[22] Richard E. Berg and David G. Stork, *The Physics of Sound* (Prentice-Hall, Englewood Cliffs, NJ, 1982), pp. 122–123.

[23] Ulrich Köpf, "Wilberforce's pendulum revisited," Am. J. Phys. **58**, 833–837 (1990).